Commun. Theor. Phys. **66** (2016) 396–400 Vol. 66, No. 4, October 1, 2016

Quasi-one Dimensional Topological Insulator: Möbius Molecular Devices in Peierls Transition*

Zhi-Rui Gong (龚志瑞),[1,2] Zhi Song (宋智),[3] and Chang-Pu Sun (孙昌璞)[2,†]

[1]College of Physics and Energy, Shenzhen University, Shenzhen 518060, China

[2]Beijing Computational Science Research Center, Beijing 100084, China

[3]Department of Physics, Nankai University, Tianjin 300071, China

(Received June 13, 2016; revised manuscript received August 4, 2016)

Abstract *We show that, assisted by the Peierls transition of lattice, as a quasi-one dimensional (Q1D) tight binding system, a Möbius molecular device can behave as a simple topological insulator. With the Peierls phase transition to form a domain wall, the solitonary zero modes exist as the ground state of this electron-phonon hybrid system, which is protected by the Z_2 topology of the Möbius strip. The robustness of the ground state prevents these degenerate zero modes from their energy spectrum splitting caused by any perturbation.*

PACS numbers: 03.65.Vf, 73.20.-r, 85.65.+h, 71.30.+h
Key words: topological insulator, Möbius boundary condition, Peierls transition

1 Introduction

Topological insulator (TI), as an exotic bulk insulator with robust metallic surfaces described by zero modes, has been extensively studied.[1−15] Many candidates of TI are of more than one dimension, such as two-dimensional HgCdTe quantum wells with helical zero modes[16−18] or the quasi-one dimensional graphene ribbon.[19−20] It seems impossible to find one-dimensional TI, since a one-dimensional system only possesses either $\boldsymbol{R}^1$ or $\boldsymbol{S}^1$ geometry respectively with the open boundary condition or periodic boundary one. However, with some lattice deformations, many-electron systems in one dimension can display spooky natures, to which the Peierls instability induced by electron-phonon interaction takes responsibility.[21−22]

In this letter, we are challenged to discovery a quasi-one dimensional (Q1D) TI, where the soliton due to Peierls transition emerges as a zero mode. In generic system with this transition, e.g., the usual polyacetylene chain by the Su–Schrieffer–Heeger (SSH) model,[23] however, the zero mode is not a ground state, thus not robust. Our present task is to force the solitonary zero mode to become a ground state by invoking a non-trivial topology of configuration spaces. This kind of systems can be implemented as experimentally accessible Möbius molecular devices,[24−30] and described as tight binding electronic models on the Möbius ladder lattice (see Fig. 1(a)). Actually, it has been shown that there exist observable topological effects, such as the topological cutoff of the transmission spectrum[31] through a non-abelian induced gauge field. The existence of the zero modes in such systems is the consequence of both the electron-phonon interaction and the Möbius boundary condition. It should be indicated that such zero modes actually are protected by the Z_2 topology of the Möbius strip in the real space, while the widely studied topological properties in solid state physics emerge in the momentum space.

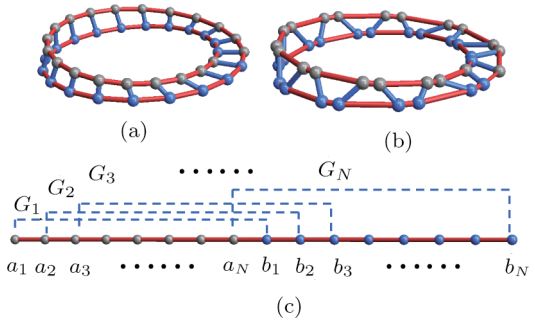

Fig. 1 (Color online) Schematic illustrations of (a) undimerized ladder with Möbius boundary condition, (b) dimerized ladder with Möbius boundary condition and (c) the corresponding one-dimensional version of Möbius ladder system with long range coupling.

2 Peierls Transition of Möbius Molecular Devices

The topological molecular device we consider consists of electrons hopping on a Möbius ladder (see Fig. 1(a)), which is a non-orientable manifold, whose edge defines a two-point bundle over $\boldsymbol{S}^1$ and thus $\mathbb{Z}^2$ topological structure. Figure 1(b) shows one of its possible lattice deformations.

*Supported by the National Natural Science Foundation of China under Grant No. 11504241 and the Natural Science Foundation of Shenzhen University under Grant No. 201551

†E-mail: cpsun@csrc.ac.cn

The corresponding Hamiltonian reads

$$H_e = \sum_{j=0}^{N-1} \boldsymbol{A}_j^\dagger \boldsymbol{M}_j \boldsymbol{A}_j - \sum_{j=0}^{N-1} \boldsymbol{J}_j \boldsymbol{A}_j^\dagger \boldsymbol{A}_{j+1} + \text{h.c.}\,, \quad (1)$$

where operator-value vector $\boldsymbol{A}_j = (a_j, b_j)^{\mathrm{T}}$ is defined in terms of the annihilation operator a_j and b_j pictured as Fig. 1(c). Here, the Möbius ladder can be regarded as a Q1D system, consisting of a-chain and b-chain with long range hopping with strength $G_j \equiv G_0$, for $j = 0, 1, \ldots, N-1$. Here, N is the site number of a-chain (b-chain). The transition matrices $\boldsymbol{M}_j = \varepsilon_j \sigma_z - G_j \sigma_x$ and $\boldsymbol{J}_j = J_j \boldsymbol{I}$ are defined by Pauli matrices σ_x, σ_y and σ_z, unity matrix $\boldsymbol{I}$, on-site energy difference $\varepsilon_j \equiv \varepsilon_0$ and hopping strength $J_j \equiv J_0$. Particularly, the boundary condition $\boldsymbol{A}_N = \sigma_x \boldsymbol{A}_0$ is taken to reflect the Möbius twist. The pure electron system is diagonalized to show two bands (Fig. 2(a)).

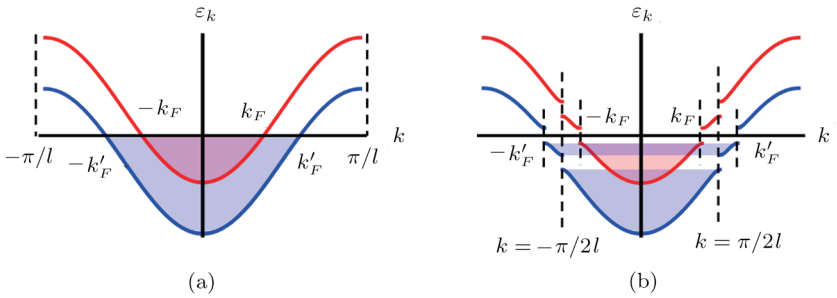

Fig. 2 (Color online) Schematic spectra of ladders without dimerization (a) and with staggered dimerization (b). The shadow regions represent the electron occupation in the energy bands.

Peierls transition induced by electron-phonon interactions in such a Q1D system, we use the Born–Oppenheimer approximation by presuming the transverse and longitudinal lattice deformations (see Fig. 3) depicted by two displacements u_j and v_j. Here, the lattice deformation is modeled as $2N$ coupled harmonic oscillators with Hamiltonian $H_p(\{u_j, v_j\})$.

There exist five dimerization patterns illustrated in Fig. 3, including three simple dimerizations and two hybrid dimerizations. Let m and l be the lattice constants along the transverse and longitudinal directions, respectively, and we can define the static uniform deformations $u_j = (-1)^j \delta$ and $v_j = (-1)^j \sigma$. They characterize the rung dimerization (Fig. 3(b)), the columnar dimerization (Fig. 3(c)), the staggered dimerization (Fig. 3(d)), vertical saw-tooth (Fig. 3(e)) and inclined saw-tooth (Fig. 3(f)).

For a given lattice deformation, we diagonalize the electronic Hamiltonian to obtain the total energy from the Born–Oppenheimer approximation. We consider the staggered dimerization (Fig. 3(b)) described by $J_j = J_0 + \alpha(l_j - l_{j-1})$ with $l_j = l + (-1)^{i+j}\sigma$, where α (β) is the rate of changes of the longitudinal (transverse) hopping. Then four separate bands are obtained as

$$\varepsilon_n(k) = (-1)^n \sqrt{\mu(\sigma) + (-1)^{\lfloor n/2 \rfloor} \nu(\sigma)}\,, \quad (2)$$

where for $n = 1, 2, 3, 4$,

$$\mu(\sigma) = G_m^2 + \Delta J^2 + 4J_0^2 \cos^2(kl + \pi/N)\,,$$
$$\nu^2(\sigma) = 4(G_0^2 \Delta J^2 + 4J_0^2 G_m^2 \cos^2(kl + \pi/N))\,,$$

for $G_m^2 = G_0^2 + \varepsilon_0^2$ and $\Delta J = 2\alpha\sigma$. $\lfloor n/2 \rfloor$ represents the integer part of $n/2$.

It follows the energy band diagram (Fig. 2(b)) that the deformation opens four gaps in the original two overlapped bands. The two gaps at $k = \pm\pi/(2l)$ are usual because they only arise from the longitudinal deformation for a-chain and b-chain, respectively. The other two gaps at Fermi momentum $k_f = \pm \arccos(G_m/2J_0)/l$ in the upper band and $k'_f = \pi/l - k_f$ in the lower band arise from the coupling between the k-states in a-chain and the $k - \pi/l$-states in b-chain with strength $\alpha\sigma G_0/2J_0$ approximately.

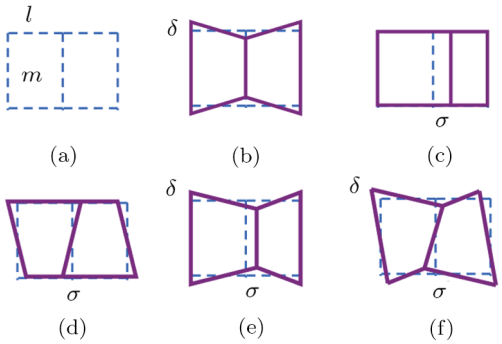

Fig. 3 (Color online) Schematic illustration of the dimerization patterns including (a) original lattice, (b) transverse, (c) columnar, (d) staggered, (e) vertical saw-tooth, and (f) inclined saw-tooth. m and l are the lengths of transverse and longitudinal directions, respectively. δ and σ denote the static deformations along transverse and longitudinal directions, respectively.

Next, we only consider the monovalent case that $2N$ electrons fill in all the negative energy levels. Apparently, the conventional gaps at $k = \pm\pi/(2l)$ have not obvious effect on the conducting properties of the elec-

trons because they are below the deformed Fermi surface. The gaps opened at Fermi surfaces may decrease the energy of the electrons by $\Delta E_e = E(\delta) - E(0)$ where $E(\delta) = \sum_{n=1,3} \int \varepsilon_n(k) \mathrm{d}k$ and $E(0)$ is the energy without dimerization. The lattice deformation also increases the energy of phonons by $\Delta E_p = 4K_l N\sigma^2 + 2K_t N\sigma^4/m^2$ where K_t and K_l are spring constants of transverse and longitudinal directions, respectively. The minimization of the total energy $\Delta E = \Delta E_p + \Delta E_e$ determines a stable configuration with a phase diagram. The above calculation is carried out for the staggered case, but repeating it for all deformations (Fig. 3) gives the total Peierls phase diagrams for the generic boundary condition (Fig. 4(a)) and Möbius one (Fig. 4(b)). Here, the parameters are chosen as $G_0 = 15\varepsilon_0$, $J_0 = 10\varepsilon_0$, $\alpha = \beta = \varepsilon_0/m$, and $l = m$.

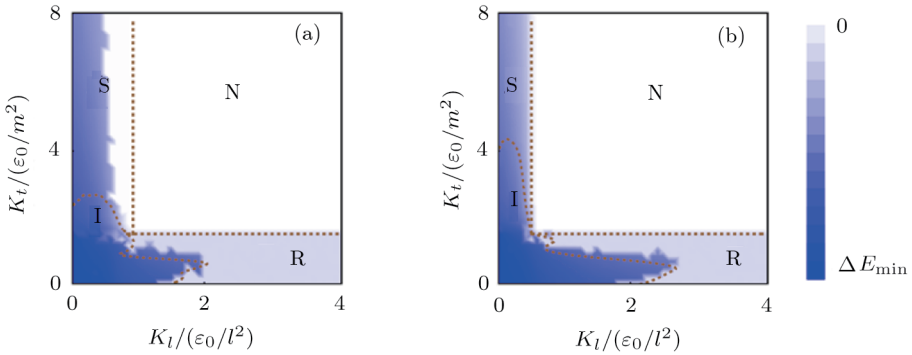

Fig. 4 (Color online) The phase diagrams of the ladder system with (a) the generic and (b) the Möbius boundary conditions, which are plotted versus (K_l, K_t) in (a) and (b), respectively. The parameters are chosen as $G_0 = 15\varepsilon_0$, $J_0 = 10\varepsilon_0$, $\alpha = \beta = \varepsilon_0/m$, and $l = m$. The distribution of the total energy ΔE versus (K_l, K_t) determines the phases boundaries, which are plotted as dashed lines. The capitalized letters "S", "I", "R", and "N", represent the staggered, the inclined saw-tooth, rung, and no dimerization, respectively.

The region of staggered dimerization pattern under the Möbius boundary condition shrinks comparing with the generic one. This fact means that metal phase is preferable for a Möbius ladder system. Therefore, the above phase diagrams show that the conducting properties can be dramatically changed when the topology of the ladder is switched. To further consider the topological effect on conducting properties, the existence of zero modes will be revisited for our Q1D system.

3 Continuum Model

We adapt the continuous field approach by regarding the Möbius ladder as a one-dimensional system with long range hopping (Fig. 1(c)). Without loss of generality, we focus on the special case $\varepsilon_0 = 0$. For a continuous field approach, it is crucial to introduce an order parameter $\Delta(x) = -4\alpha u(x)$, where $u(x)$ is the continuous limit of displacements $(-1)^j u_j$.

The Hamiltonian of continuum model $H = H_e + H_p$ contains the phonon part

$$H_p = \int_{-L}^{L} \mathrm{d}x \Big\{ \frac{K_l}{8\alpha^2 l} \Delta^2(x) + \frac{M}{32\alpha^2 l} \dot{\Delta}^2(x) + \frac{K_t}{4^6 m^2 \alpha^4 l} [\Delta(x+L) - \Delta(x)]^4 \Big\}, \tag{3}$$

and the electron part

$$H_e = \int_{-L}^{0} \mathrm{d}x \Phi^\dagger(x) \mathscr{H}(x) \Phi(x),$$

where M is the mass of the single particle and $L = Nl$ is the length of the a-chain (b-chain), which approaches infinity at the end of calculation. In the electron part, the hopping electron could be described with a 4-component spinor $\Phi(x) = [\phi_1(x), \phi_2(x), \phi_3(x), \phi_4(x)]^{\mathrm{T}}$. Physically, $\phi_1(x)$ ($\phi_3(x)$) and $\phi_2(x)$ ($\phi_4(x)$) respectively represent the left-traveling waves and right-traveling waves in a-chain (b-chain). In this spinor representation, the Hamiltonian density is expressed as σ_x, σ_y and σ_z,

$$\mathscr{H} = \begin{bmatrix} \mathrm{i}v_f \sigma_z \partial_x + \Delta(x)\sigma_x & G(x) \\ G(x) & \mathrm{i}v_f \sigma_z \partial_x + \Delta(x+L)\sigma_x \end{bmatrix}, \tag{4}$$

where $v_f = 2lJ_0$, and $G(x) = G_0 + \beta[\Delta(x) - \Delta(x+L)]^2/(32m\alpha^2)$ is effective coupling between the a-chain and b-chain.

To reflect the Möbius boundary condition in our Q1D model (Fig. 1(c)), we take the period $2L$ for boundary conditions $\Phi(x+2L) = \Phi(x)$ rather than L for the generic case. With this boundary condition, we solve the Bogoliubov-de Gennes (BdG) equation $\mathscr{H}\Phi_i(x) = \varepsilon_i \Phi_i(x)$, where i represents the i-th energy band of the spectrum and $\Phi_i(x) = [\phi_1^i(x), \phi_2^i(x), \phi_3^i(x), \phi_4^i(x)]^{\mathrm{T}}$. At zero temperature, the order parameter $\Delta(x)$ satisfies the self-consistent equations

$$\frac{K_l}{4\alpha^2 l}\Delta(x) - \frac{K_t}{4^5 m^2 \alpha^4 l}(\Delta(x+L) - \Delta(x))^3 = \begin{cases} \sum_i 2\mathrm{Re}\,[\phi_1^{i,*}(x)\phi_2^i(x)], & \text{for } x \le 0, \\ \sum_i 2\mathrm{Re}\,[\phi_3^{i,*}(x)\phi_4^i(x)], & \text{for } x > 0, \end{cases} \tag{5}$$

which were obtained by the functional variation of $E(\Delta(x)) = \sum_i \varepsilon_i + H_p$ with respect to $\delta\Delta(x)$ and $\delta\Delta(x+L)$. The sum is over the energy levels below the Fermi surface.

4 Zero Modes for Topological Insulator

As we show as follows, some solutions of the above BdG equation can exist as zero modes. When they happen to be ground state and robust under external perturbations, the Möbius system then becomes a topological insulator.

In the following, we only consider the case $K_l \ll K_t$. In this case, three dimerization patterns of rung (Fig. 3(b)), vertical-saw tooth (Fig. 3(e)) and inclined saw-tooth (Fig. 3(f)) occur rarely. Thus we only need to compare the energy of staggered with columnar one. Let us first revisit Möbius ladder system with the staggered dimerization characterized by $\Delta(x) = -\Delta(x+L)$. In this phase, the order parameters in a- and b-chains are opposite and display a Peierls phases domain wall. We also notice that the columnar dimerization to be compared is characterized by $\Delta(x) = \Delta(x+L)$.

For the staggered case, we assume a kink deformation $\Delta(x) = \Gamma\tanh(x/\xi)$ with $\xi = v_f/\Gamma$, which is so small that the effective coupling between the a- and b-chain as $G(x) \approx G_0$. In this sense, the BdG equation is written as

$$\begin{bmatrix} \mathrm{i}v_f\sigma_z\partial_x + \Delta(x)\sigma_x & G_0 \\ G_0 & \mathrm{i}v_f\sigma_z\partial_x + \Delta(x+L)\sigma_x \end{bmatrix} \Phi_i(x) = \varepsilon_i\Phi_i(x)\,. \tag{6}$$

To solve the above equation, we apply a unitary transformation as $\Psi_i(x) = U\Phi_i(x)$, where the transformed wavefunction are defined as

$$\Psi_i(x) = [\varphi_1^i(x), \varphi_2^i(x), \varphi_3^i(x), \varphi_4^i(x)]^{\mathrm{T}}$$

and the unitary matrix is

$$U = \frac{1}{\sqrt{2}}\begin{bmatrix} 1 & \mathrm{i} & 0 & 0 \\ 1 & -\mathrm{i} & 0 & 0 \\ 0 & 0 & 1 & \mathrm{i} \\ 0 & 0 & 1 & -\mathrm{i} \end{bmatrix}. \tag{7}$$

After the transformation, the BdG equation for $\Psi_i(x)$ becomes

$$\begin{bmatrix} \mathrm{i}v_f\sigma_x\partial_x - \Delta(x)\sigma_y & G_0 \\ G_0 & \mathrm{i}v_f\sigma_x\partial_x - \Delta(x+L)\sigma_y \end{bmatrix} \Psi_i(x) = \varepsilon_i\Psi_i(x)\,. \tag{8}$$

As the solutions of the BdG equation with energy $\varepsilon_i = 0$, two degenerate solitonary states $\varphi^i_{1(3)} = (\phi^i_{1(3)} + \mathrm{i}\phi^i_{2(4)})/\sqrt{2}$ and $\varphi^i_{2(4)} = (\phi^i_{1(3)} - \mathrm{i}\phi^i_{2(4)})/\sqrt{2}$ (illustrated in Fig. 5(a) as the middle line $\varepsilon_s = 0$) can be found as one with non-vanishing components $\varphi^s_2(x) = \varphi^s_3(x) = F^s_+(x)$, and another with non-vanishing components $\varphi^s_2(x) = -\varphi^s_3(x) = F^s_-(x)$ for

$$F^s_\pm(x) = \sqrt{\frac{1}{2\xi}}\exp\Big(\pm\mathrm{i}\frac{G_0}{v_f}x\Big)\mathrm{sech}\Big(\frac{x}{\xi}\Big)\,. \tag{9}$$

These solitonary states are the zero modes existing at the midgap. Since there is no such solitonary state in the generic ladder, the existence of the solitons is absolutely topological effect.

We note that the another two bands $\varepsilon^\pm_v = -\sqrt{(v_fk \pm G_0)^2 + \Gamma^2}$ (illustrated in Fig. 5(a) as two overlapped shadowed domains) fully occupied by the electrons correspond to eigen functions

$$\varphi^{v,\pm}_1(x) = \pm\varphi^{v,\pm}_4(x) = \mathrm{i}\exp(-\mathrm{i}kx)/2\sqrt{L}\,,$$
$$\varphi^{v,\pm}_2(x) = \pm\varphi^{v,\pm}_3(x) = F^v_\pm(x)\exp(-\mathrm{i}kx)/2\sqrt{L}\,,$$

where

$$F^v_\pm(x) = \frac{\Gamma}{\varepsilon^\pm_v}\Big[\tanh\frac{\Gamma x}{v_f} + \mathrm{i}\frac{(v_fk \pm G_0)}{\Gamma}\Big] \tag{10}$$

represents a deviation from a plane wave in the kink order. Then, it follows from the self-consistent equations Eq. (5) that

$$\Gamma \approx \Delta_0\exp(-B\Delta_0^2)\,, \tag{11}$$

where $\Delta_0 = W\exp(-A)$ is the order parameter for one-dimensional uniformly dimerized system, $W = 2v_fk_f$, $A = v_f\pi K_l/8\alpha^2 l$, and $B = v_f\pi K_t/2^7m^2\alpha^4 l$ with k_f is the Fermi momentum.

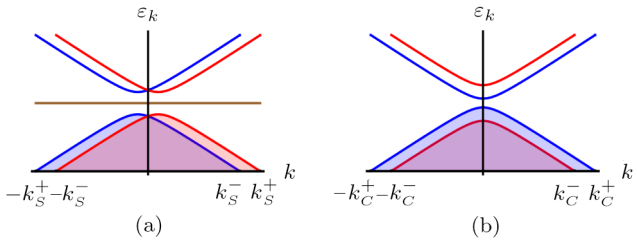

Fig. 5 (Color online) Schematics of the energy spectra of the valence bands under (a) staggered and (b) columnar dimerizations, where $k_S^\pm = k_f \mp G_0/v_f$ and $k_C^\pm = \sqrt{G_0^2 + v_f^2k_f^2 \pm 2G_0\sqrt{v_f^2k_f^2 + \Gamma^2}}/v_f$. The shadow regions represent the electron occupation in the energy bands, and the brown straight line represents the solitonary states.

Moreover, we can further prove that the above solitonary states are the ground states. To this end we calculate the total energy of the electron-phonon system E_T^S according to the phase shift[22] of the eigen-functions $\theta^\pm(k) = \theta^\pm_{-\infty}(k) - \theta^\pm_{+\infty}(k) = \pi + 2\arctan(v_fk \pm G_0)/\Gamma$. A straightforward algebra explicitly gives

$$E_T^S = E_T^C + \frac{4\Gamma}{\pi} - \frac{G_0^2}{v_fk_f} + \delta(K_t)\,, \tag{12}$$

where E_T^C is the total energy for the columnar dimerization (Fig. 3(c)), and $\delta(K_t) = 13K_t\Gamma^3v_F/(3\times 4^4m^2\alpha^4 l)$ results from the coupling between the a- and b-chain. The second term in E_T^S is usual energy increment due to the exitance of solitonary states. The third term in E_T^S results from the difference in the total energies in two filling ways. One corresponds to the staggered dimerization (Fig. 5(a)) with two lower bands $-\sqrt{(v_fk \pm G_0)^2 + \Gamma^2}$ occupied by

electrons, while the other corresponds to columnar one (Fig. 5(b)) with two lower bands $\pm G_0 - \sqrt{(v_f k)^2 + \Gamma^2}$ occupied. For the latter the energy of electrons increases because a part of electrons are forced to occupy higher energy levels. If G_0 is so large that $\delta E = E_T^S - E_T^C$ is negative, the ground state of the Möbius ladder system corresponds to the staggered dimerization rather than the columnar one. In this case the solitonary states are zero modes existing as the ground state.

Actually, the topology of the system can protect the solitonary state from external perturbations. For example, when the soliton propagates along the longitudinal directions without spreading, the energy increment caused by moving soliton with velocity v_s from the time evolution of order parameter $\Delta(x,t) \equiv \Gamma \tanh(x - v_s t)/\xi$ is $\Delta E_s = M v_s^2 \Gamma^3/(24 v_f \alpha^2 l)$, which could be much smaller than the exciting energy δE. Since the moving soliton is robust and charged, the Möbius ladder with staggered dimerization is actually electrically conductive.

5 Conclusion

We have shown that the Möbius molecular devices assisted by Peierls instability could be regarded as the simplest example of topological insulator. When the Möbius boundary condition is applied to the ladder system, the solitonary solutions emerge in such a quasi-one dimensional system as ground state in the Peierls phases domain wall. The existence of the zero modes is the consequence of both the electron-phonon interaction and the Möbius boundary condition. The electron-phonon interaction causes the dimerization and the transporting solitonary states. The Möbius boundary condition just guarantees that the solitonary solutions are the ground state. Such zero modes actually are protected by the Z_2 topology of the Möbius strip in the real space, while the widely studied topological properties in solid state physics emerge in the momentum space. As the charged zero modes propagating without spreading, the conducting properties of the Möbius molecular devices are pretty dramatic for topological insulator.

Acknowledgments

The authors thank Nan Zhao for helpful discussion.

References

[1] M.Z. Hasan and C.L. Kane, Rev. Mod. Phys. **82** (2010) 3045.
[2] X.L. Qi and S.C. Zhang, Phys. Today **63** (2010) 33.
[3] J.E. Moore, Nature (London) **464** (2010) 194.
[4] X.L. Qi and S.C. Zhang, Rev. Mod. Phys. **83** (2011) 1057.
[5] S.C. Zhang, Physics **1** (2008) 6.
[6] L. Fu, C.L. Kane, and E.J. Mele, Phys. Rev. Lett. **98** (2007) 106803.
[7] L. Fu and C.L. Kane, Phys. Rev. B **76** (2007) 045302.
[8] J.C.Y. Teo, L. Fu, and C.L. Kane, Phys. Rev. B **78** (2008) 045426.
[9] J.E. Moore, Y. Ran, and X.G. Wen, Phys. Rev. Lett. **101** (2008) 186805.
[10] X.L. Qi, T.L. Hughes, and S.C. Zhang, Phys. Rev. B **78** (2008) 195424.
[11] A.M. Essin and J.E. Moore, Phys. Rev. B **76** (2007) 165307.
[12] H. Obuse, *et al.*, Phys. Rev. B **78** (2008) 115301.
[13] Y. Ran, Y. Zhang, and A. Vishwanath, Nat. Phys. **5** (2009) 298.
[14] J. Li, *et al.*, Phys. Rev. Lett. **102** (2009) 136806.
[15] A. Bermudez, *et al.*, Phys. Rev. Lett. **102** (2009) 135702.
[16] B.A. Bernevig, T.L. Hughes, and S.C. Zhang, Science **314** (2006) 1757.
[17] M. König, *et al.*, Science **318** (2007) 766.
[18] J.E. Moore and L. Balents, Phys. Rev. B **75** (2007) 121306(R).
[19] Z.L. Guo, *et al.*, Phys. Rev. B **80** (2009) 195310.
[20] Z.L. Guo, Z.R. Gong, and C.P. Sun, arXiv:0904.2231 (2009).
[21] W.P. Su, J.R. Schrieffer, and A.J. Heeger, Phys. Rev. Lett. **42** (1979) 1698.
[22] H. Takayama, Y.R. Lin-Liu, and K. Maki, Phys. Rev. B **21** (1980) 2388.
[23] W.P. Su, J.R. Schrieffer, and A.J. Heeger, Phys. Rev. Lett. **42** (1979) 1698.
[24] V. Balzani, A. Credi, and M. Venturi, *Molecular Devices and Machines: A Journey Into the Nanoworld*, Wiley-VCH Verlag GmbH & Co. KGaA, Weinheim (2003).
[25] A. Nitzan and M.A. Ratner, Science **300** (2003) 1384.
[26] K. Burke, R. Car, and R. Gebauer, Phys. Rev. Lett. **94** (2005) 146803.
[27] C. Zhang, *et al.*, Phys. Rev. Lett. **92** (2004) 158301.
[28] M.J. Comstock, *et al.*, Phys. Rev. Lett. **99** (2007) 038301.
[29] A. LaMagna and I. Deretzis, Phys. Rev. Lett. **99** (2007) 136404.
[30] C.Q. Wu, J.X. Li, and D.H. Lee, Phys. Rev. Lett. **99** (2007) 038302.
[31] N. Zhao, *et al.*, Phys. Rev. B **79** (2009) 125440.